Journal of African Earth Sciences 113 (2016) 181–193

Contents lists available at ScienceDirect

Journal of African Earth Sciences

journal homepage: www.elsevier.com/locate/jafrearsci

Differential dissolution susceptibility of Paleocene foraminiferal assemblage from Farafra Oasis, Egypt

Orabi H. Orabi*, Amr S. Zaky

University of Menoufia, Faculty of Science, Department of Geology, Egypt

ARTICLE INFO

Article history:
Received 14 June 2014
Received in revised form
28 October 2015
Accepted 2 November 2015
Available online 6 November 2015

Keywords:
Egypt
Farafra Oasis
Paleocene
Dissolution

ABSTRACT

Four inferred carbonate dissolution intervals are recognized at North Gunna section within the Dakhla and Esna formations (Paleocene) of the Farafra Oasis of Egypt as the following: 1) at the Danian/Selandian boundary (P3a/P3b), 2) at the upper part of *Acarinina soldadoensis/Globanomalina pseudomenardii* Subzone (P4c), 3) at the upper two third of the *Morozvella velascoenis* P5 Biozone and 4) at the Paleocene/Eocene boundary of *Morozovella velascoensis/Morozovella aragonensis-Morozovelia subbotinae* (P5/E5), where the P/E boundary is marked by major hiatus.

The essential indicators of dissolution within the four intervals samples are low P/B ratios, high relative abundance of the agglutinated taxa, high relative abundance of calcareous taxa resistant to dissolution, especially *Lenticulin, Cibicidoides* and *Anomalinoides* and low relative abundance of susceptible calcareous taxa, such as unilocular, uniserial and biserial taxa for the benthics and non-muricate taxa for the planktonic, associated with the high percentage of organic carbon.

The probably factors may contribute to the dissolution of planktonic foraminiferal tests in the four intervals of dissolution at the Farafra Oasis is that acidity produced by the degradation of organic matter promotes dissolution in sediment pore waters.

1. Introduction

In previous times, the Pg/E boundary publication focused on the litho-, bio-, chemostratigraphy, mineralogy and sedimentology of the Esna Formation at different stratigraphic section along the Nile Valley (e.g., Dababiya, Qreiya, Owaina and Kilabiya sections) to define the Global Stratotype-Section and Point (GSSP) of the Pg/E boundary. The dissolution of planktonic and benthic foraminifera of the Farafra Oasis was relatively neglected, in spite of the fact that it represents part of the stratigraphic sequence in the Western Desert.

A basic assumption in palaeoenvironmental studies is that fossil assemblages reflect the initial biocoenosis and underlying environmental signals (e.g. Berger and Diester-Haass, 1988; Nolet and Corliss, 1990; Casieri and Carboni, 2007). However the planktonic and benthic foraminifera are vulnerable to dissolution, but planktonic foraminifera are generally more vulnerable than benthic foraminifera because the former typically have porous chamber walls designed to maintain buoyancy in surface waters. Thus leading to depressed P/B ratios (Berger, 1967, 1970, 1973; Peterson and Prell, 1985; Dittert et al., 1999). Benthic foraminifera are in general more dissolution resistant than planktonics, both in modern (Thunell, 1976; Peterson and Prell, 1985; Dittert et al., 1999) and fossil assemblages (Petrizzo et al., 2008; Nguyen et al., 2009). The relative abundance of benthic foraminifers may serve as an index for carbonate dissolution at deep water sites (Schlanger and Douglas, 1973; Thunell, 1976).

The majority of previous studies on foraminiferal dissolution focused on the possible influence of calcite dissolution on the size of calcareous foraminifera (Corliss, 1979; Corliss and Honjo, 1981); factors controlling the dissolution of the assemblages (e.g., de Vernal et al., 1992; Herrero and Canales, 2002); dissolution characteristics of foraminifera (Berner et al., 1976; Peterson and Prell, 1985) and records of dissolution in foraminiferal assemblages, at different levels and in different places (e.g., Stephen and Buzas, 2005; Tobin et al., 2005).

This study aims to investigate the effects of differential dissolution on the composition of foraminiferal assemblages. More specifically, we examine differential dissolution between types of planktonic foraminifera, changes in P/B ratio (%P), the number of planktonic (PF) and benthic foraminifera (BF) and the morphologic

* Corresponding author.
E-mail address: Oraby1952@yahoo.com (O.H. Orabi).

http://dx.doi.org/10.1016/j.jafrearsci.2015.11.004
1464-343X/© 2015 Published by Elsevier Ltd.

compositions of foraminiferal assemblages affected by dissolution. Through this we assess the value of the commonly used foraminiferal dissolution indices, P/B ratios, which are generally considered to be the best indicators of taphonomic dissolution in Paleocene studies of the North Gunna section. Results from this study are used for the first time in the Farafra Oasis (Fig. 1), where the dissolution is observed in the foraminiferal assemblages of the Dakhla and Esna formations.

2. Regional setting

The Farafra Oasis is one of the five major oases of the Western Desert of Egypt. It lies 300 Km west of Assiut, 500 Km southwest of Cairo, 200 Km southwest of Bahariya Oasis and 300 Km northwest of Dakhla Oasis.

The Farafra depression is of irregular triangular shape with its apex to the north; its breadth increases as one goes south. It is surrounded from three sides by escarpments 120–160 m higher than the floor. It is open to the south where its floor gently and gradually merges into the general plateau of the desert to the south and southwest. Only the eastern escarpment continues southwards to join the northwestern escarpment of the Dakhla Oasis (Fig. 2).

The floor of the depression is mainly composed of chalk in the northern half, slopes gently from south to north. Its monotony is broken by few hills and dune area. A group of three hills lies about 15 km north of Qasr El Farafra. One of these hills called North Gunna. The El- Quess Abu Said Plateau forms the northwestern and western limits of the depression. It is bordered on northwestern side by another depression.

From 90 km south of Farafra, the Khoman Chalk loses gradually its carbonate character and replaced by shale facies (Dakhla Formation). The shales and overlying Paleocene carbonate (Tarawan Formation) make a steep scarp overlooking Abu Munqar miniature oasis in the west and continues southward to bind the Dakhla

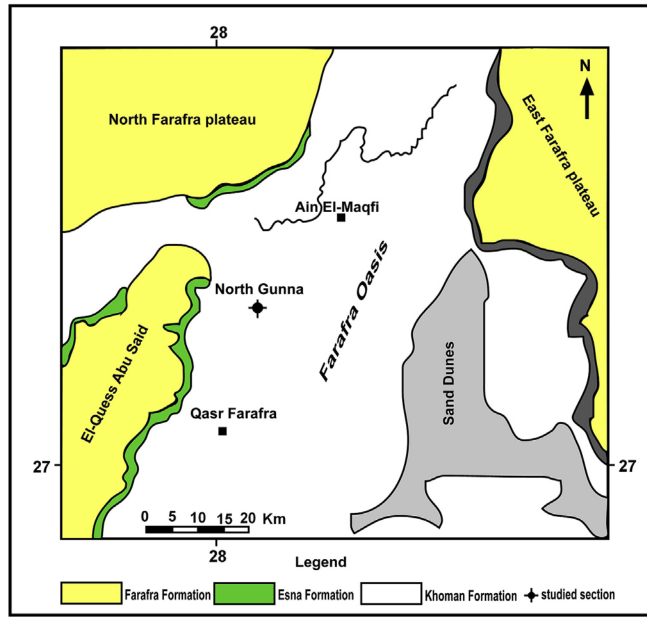

Fig. 2. Geological map of the Farafra Oasis (Western Desert of Egypt).

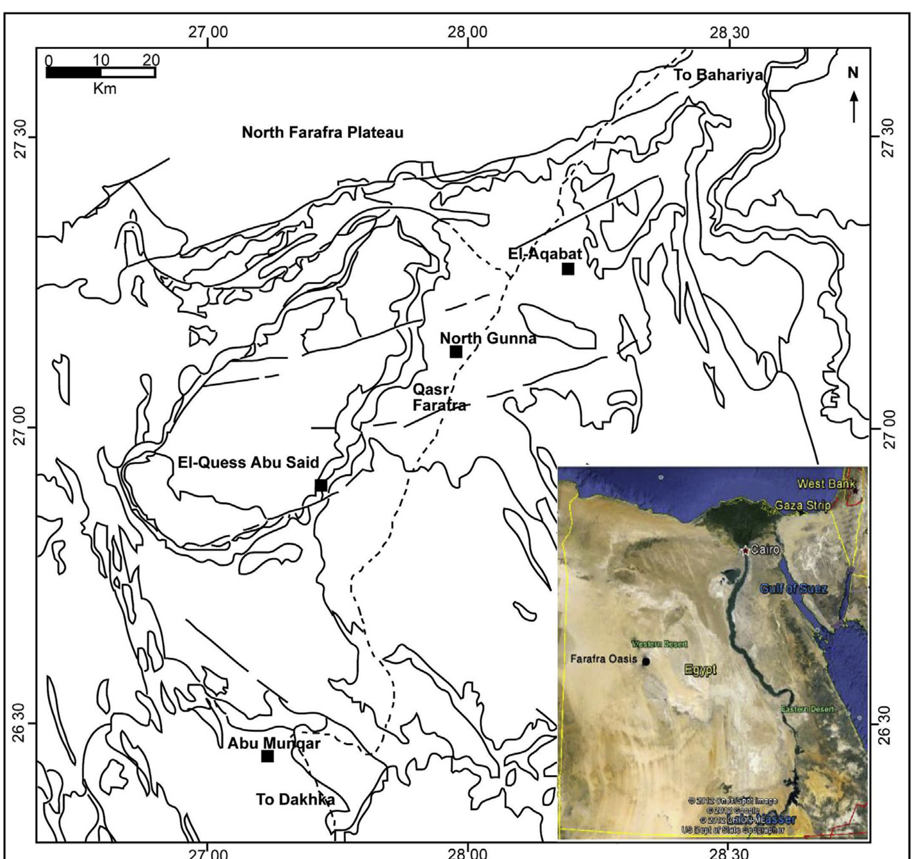

Fig. 1. Locality map.

depression lying to the south (Issawi et al., 1999).

The Abu Munqar is situated within the lower units of the Dakhla. The encroachment of the area by the eastern dunes of the Great Sand Sea lying to its west-led the desertification of the oasis and its abandonment.

The stratigraphic succession of the North Gunna section of the Farafra Oasis exposes Upper Cretaceous, Paleocene, and Lower Eocene strata. The carbonates are known as the Khoman Formation, compose most of the Maastrichtian and early Paleocene strata in the north of the oasis; these changes progressively southward into shales (Dakhla Formation), with a persistent unit of white chalk at their top (Tarawan Formation). The Tarawan supports in turn a thick sequence of green gypseous shales (Esna Formation), capped by buff biogenic limestones packed with alveolines; the latter are called the Farafra Limestone.

2.1. The Khoman Formation (El-Akkad and Issawi, 1963)

In the present study, planktonic foraminiferal investigations assigned the Khoman Formation to the Maastrichtian-Danian. The North Gunna section starts with Khoman Chalk of about 10 m thick, where Barthel and Herrmann-Degen (1981) pointed out that the Khoman Formation represents a fairly shallow marine suite on the swell of the Bahariya Arch.

2.2. The Dakhla Formation (Said, 1962)

The Dakhla Formation marks the Lower Paleocene sequence exposed in the study area, and is of particular interest because of its rhythmic deposition of mudstones and siltstones. At the upper part of the Dakhla Formation a glauconitic bed is present and the formation attains a thickness of about 8 m.

2.3. The Tarawan Formation (Awad and Ghobrial, 1965)

The Tarawan Formation is composed of yellowish white to light grey argillaceous limestone and marly limestone with thin intercalations of clays at the lower part. The base of the Tarawan Formation is piped by Callianassid burrow. A bioturbated conglomeratic bed with phosphatic pebbles, vertebrate remains at the base of the formation which may belong to sessile organisms marks a hiatus between Dakhla and Tarawan formations. It attains a thickness of about 6 m and the contact delineates a break in sedimentation at the top of the Dakhla Formation.

2.4. The Esna Formation (Beadnell, 1905; emended by Said, 1962)

The Esna Formation conformably overlies the Tarawan Formation and underlies the Farafra limestone. The Esna Formation is made up of grey shale in the basal part and green to violet shale in its top part and it attains a thickness of about 39 m. Malak et al. (1977) suggested that these shales were deposited in stagnating, reducing, slightly alkaline water with an upper oxygenated surface zone in which green algae lived and acted as the main source of organic matter.

3. Material and methods

3.1. Foraminiferal study

Samples were obtained from fresh unweather bedrock after removing surface contamination. A total 75 samples were analyzed for this study.

Approximately 80 g of sediment were dried at 50–60 °C for 24 h or longer and afterwards soaked in a Na_2CO_3 solution for a day. After disintegration, the samples were washed over a 63 μm sieve and dried at 50–60 °C; this treatment was repeated twice whenever the washed residues remained somewhat aggregated. After complete disaggregation, the 125–630 μm size fraction was used in quantitative foraminiferal studies, especially those on the lower Paleogene of North Africa (e.g., Speijer and Schmitz, 1998; Guasti et al., 2005). A representative split for quantitative analysis (approximately >300 planktonic and benthic specimens) was obtained from the 125–630 μm fraction using a microsplitter. From these splits, all planktonic and benthic specimens were picked, identified, counted and permanently stored on micropaleontological slides (Table 1). The Scanning Electron Microscope (SEM) imaged specimens are part of the private collection of the senior author, fresh samples and residues are stored at the Department of Geology, University of Menoufia (Plates 1–3).

Preservation of planktonic foraminifera for this section is generally good although dissolution of calcite shell is evident in some samples. Then the numbers of specimens of all samples were counted, together with the number of specimens belonging to each architectural type (five main types of architecture are distinguished: unilocular, uniserial, biserial, planispiral and trochospiral) (Table 1). The results from these counts were used to calculate P/B ratios, the number and percentage of planktonic and benthic (Fp and %Fp, Fb and %Fb, respectively), and agglutinated percentage. The calculations are: $P/B = PF/(PF + BF)$; $\%Fp = Fp/(Fp + PF)$; $\%Fb = Fb/(Fb + BF)$.

3.2. Determination of total organic carbon content (TOC)

The total organic carbon content was determined for 75 rock samples using a Hochtemperatur-TOC/TNb-Analysator (Liqui TOC) after decarbonating. The whole rock samples were analysed for TOC concentrates. About 200 mg pulverised sample was used for this analysis. Carbonate was removed by treatment with 10% aqueous hydrochloric-acid. The residual materials were used for the determination of TOC by combustion analysis of temperatures in excess of 850 C°. The evolved gas (CO_2) was measured quantitatively and simultaneously by infrared detectors and recorded as percentage of carbon.

4. Planktonic foraminiferal zonations

Stratigraphic distribution of the planktonic foraminifera in the studied section at Gebel Gunna section is shown in text-Fig. 3. The zonal scheme of Caron (1985), Li and Keller (1998a, b), Li et al. (1999) and Arz and Molina (2002) is used here for the Cretaceous planktonic foraminiferal zones. Meanwhile, the planktonic foraminiferal zonation of Berggren et al. (1995) and Berggren and Pearson (2005) is using for the Paleocene zones. Planktonic foraminiferal biostratigraphic zones suggested in this work cover a time interval ranging from the Late Maastrichtian to the Early Eocene. In the present study, the recorded Cretaceous biozones at Gebel Gunna section are *Pseudogumbelina palpebra* (CF2), where the latest Cretaceous *Plummerita hantkeninoides* (CF1) and earliest Paleocene *Guembelitria cretacea* (P0) were not recorded in the studied sections, although there are no recognizable unconformity signs.

In the present study, the recorded Paleocene planktonic foraminiferal biozones are arranged in stratigraphic order from older to younger as follows; *Praemurica uncinata* Zone (P2) of Early Danian, *Morozovella angulata* subzone (P3a) of Late Danian, *Igorina albeari* Zone (P3b) of Early Selandian, *Parasubbotina variospira* Subzone (P4a) of Late Selandian, *Acarinina subsphaerica* subzone (P4b) of Latest Selandian-Early Thanetian, *Acarinina soldadoensis*/*Globanomalina pseudomenardii* Subzone (P4c) of Early Thanetian and *Morozovella velascoenis* Zone (P5) of Latest Thanetian.

Table 1
The distribution of architectural groups of benthic assemblages and planktonic foraminifera counts in the studied samples.

Formation	Biozones	Sample no.	Benthic numbers						Planktic number
			Unil-ocular	Uni-serial	Bise-rial	Planis-spiral	Tochospir.	Aggluti-nated	
Esna	*M. velascoensis*	69	Barren						
	P5	68	5	14	7	52	9	108	17
		67	Barren						
		66	–	–	–	76	–	72	33
		65	4	9	4	53	3	60	60
		64	–	–	–	4	–	–	–
		63	14	14	–	75	12	45	84
		62	8	4	10	50	10	87	105
		61	7	–	7	32	–	99	15
		60	–	–	–	42	12	46	28
	A. soldadoensis	59	Barren						
	P4c	58	–	–	–	55	–	75	28
		57	–	4	–	78	18	41	60
Tarawan	*A. subsphaerica* P4b	56	–	–	–	45	7	39	72
		55	–	–	–	30	3	2	30
		54	–	–	–	2	–	–	–
		53	–	–	–	2	–	–	–
		52	–	5	–	–	–	6	30
		51	–	4	–	41	–	37	12
		50	–	2	3	56	6	27	3
		49	–	–	–	2	–	–	–
		48	–	–	–	3	–	–	–
		47	–	4	3	58	–	–	36
		46	–	–	–	2	–	–	–
		45	2	–	2	26	2	–	39
		44	4	3	–	14	–	8	27
		43	–	–	4	17	3	–	18
		42	–	3	–	5	–	24	108
	G.variospira P4a	41	–	3	–	21	–	6	105
		40	–	2	–	43	–	12	99
Dakhla	*I. albeari* P3b	39	–	–	–	57	–	23	87
		38	–	–	–	54	–	17	99
		37	–	–	–	65	–	6	100
		36	–	–	–	56	4	4	87
		35	–	–	–	60	–	5	80
		34	–	–	–	55	–	5	92
		33	–	3	6	57	7	6	87
	M. angulata	32	Barren						
	P3a	31							

Table 1 (*continued*)

Formation	Biozones	Sample no.	Benthic numbers						Planktic number
			Unil-ocular	Uni-serial	Bise-rial	Planis-spiral	Tochospir.	Aggluti-nated	
		30							
		29							
		28							
		27	–	9	–	22	–	76	30
		26	2	21	–	50	3	70	17
		25	–	–	–	–	–	4	–
		24	–	20	–	40	–	74	43
		23	–	58	–	89	–	36	102
		22	14	47	–	87	–	17	90
		21	11	–	–	–	–	–	–
		20	20	14	–	47	–	12	74
	P. uncinata	19	4	3	–	38	–	24	93
	P2	18	2	5	3	39	3	42	102
		17	–	–	2	16	–	6	45
		16	4	6	3	44	2	30	75
		15	–	–	2	33	–	16	66
		14	2	3	2	29	–	3	75
		13	7	17	8	90	4	18	162
		12	2	2	4	50	2	–	198
		11	4	3	–	34	–	12	138
		10	9	17	4	78	–	3	166
		9	–	3	–	30	–	6	42
		8	5	3	2	28	2	6	165
		7	12	5	–	49	–	9	102
		6	–	–	–	48	–	6	108
		5	18	–	12	52	–	24	39
Khoman		4	–	–	–	70	–	9	111
		3	11	10	–	59	–	3	102
	P. palbepra	2	Not studied						
	CF2	1							

The P/E boundary is marked by major hiatus recorded at North Gunna section. This boundary lies within the Esna Formation at *Morozovella velascoensis*/*Morozovella aragonensis-Morozovelia subbotinae* (P5/E5) zonal boundary with major hiatus that well documented by the absence of the E1, E2, E3 and E4 zones of Early Eocene age. This finding is not in line with the foraminiferal assemblage studied from Dababiya Quarry section near Luxor, Egypt. This locality hosts the Global boundary Stratotype Section and Point (GSSP).

5. Interval of dissolution

5.1. First interval of dissolution

The benthic foraminiferal assemblage of the upper part of *M. angulata* Biozone (P3a) is characterized by the richness of arenaceous foraminifera as *Dorothia conulus*, *Vulvulina colei, Migros midwayensis*, *Gaudryina soldadoensis*, *Pseudoclavulina amorpha* and *Pseudoclavulina globulifera* (Plate 2). Meanwhile, the recorded calcareous benthic assemblage is rare diversified, moderate preserved and represented by *Lagena apiculata*, *Stilostomella gracillima*, *Cibicidoides praecursoria* and *Gyroidinoides subangulata* (Plate 3). It is worth mention that most planktonic foraminiferal numbers of samples 26–27 are rare and show dissolution pattern overlain by barren interval at the upper part of this biozone (Table 2).

5.2. Second interval of dissolution

The benthic foraminiferal assemblage recorded in *A. soldadoensis*/*Globanomalina pseudomenardii* Subzone (P4c) (sample 57–58) is dominated by rich agglutinated genera specially *Dorothia* and *Valvulina* and very scars of planktonic forams. The agglutinated genera represented by *Dorothia bulletta*, *D. conulus*, *Dorothia glabrella*, *Vulvulina colei*, *Vulvulina advena*, *Marsonella oxycona*, *Textularia* cf. *plummerae*, *Psammosphaera fusca*, *Miliammina* sp., *P. amorpha* and *P. globulifera* (Plate 2). Meanwhile, the calcareous forams are few and represented by *Lenticulina pseudomamilligera*, *Lenticulina oligostegia*, *Anomalinoides affinis*, *S. gracillima* and *G. subangulata* (Plate 3). The planktonic foraminifera are few and show dissolution pattern overlain by barren interval at the upper part of this biozone (Table 3).

5.3. Third interval of dissolution

At the upper two third of *M. velascoensis* Biozone (P5) the dissolution pattern is well recognized at sample 66 (Fig. 4) which represented by high content of arenaceous forms as *D. bulletta*, *D. conulus*, *D. glabrella*, *Vulvulina colei*, *V. advena*, *M. oxycona*, *Textularia* cf. *plummerae*, *Textularia punjabensis*, *P. fusca*, *Haplophragmoides excavatus*, *P. amorpha*, *P. globulifera* and *Trochammina uniatensis*. The calcareous one is moderate content and some forams of planktonic genera show dissolution at last chamber (Plate 1). Thus dissolution leads to a decrease in diversity and the absolute number of specimens also decreased with the decreasing number of taxa (Table 4). It is worth mention that the top of this biozone is overlain by barren interval (sample 67).

5.4. Fourth interval of dissolution

The planktonic foraminifera are very few in the Paleocene/Eocene boundary of *M. velascoensis*/*Morozovella aragonensis-M. subbotinae* (P5/E5) (sample 68) and overlain by barren interval (sample 69). The planktonic foraminifera are much more vulnerable to dissolution than benthic foraminifera, leading to depressed P/B ratios at this interval (Fig. 4). The calcareous benthic forams are represented by moderate content of *L. oligostegia*,

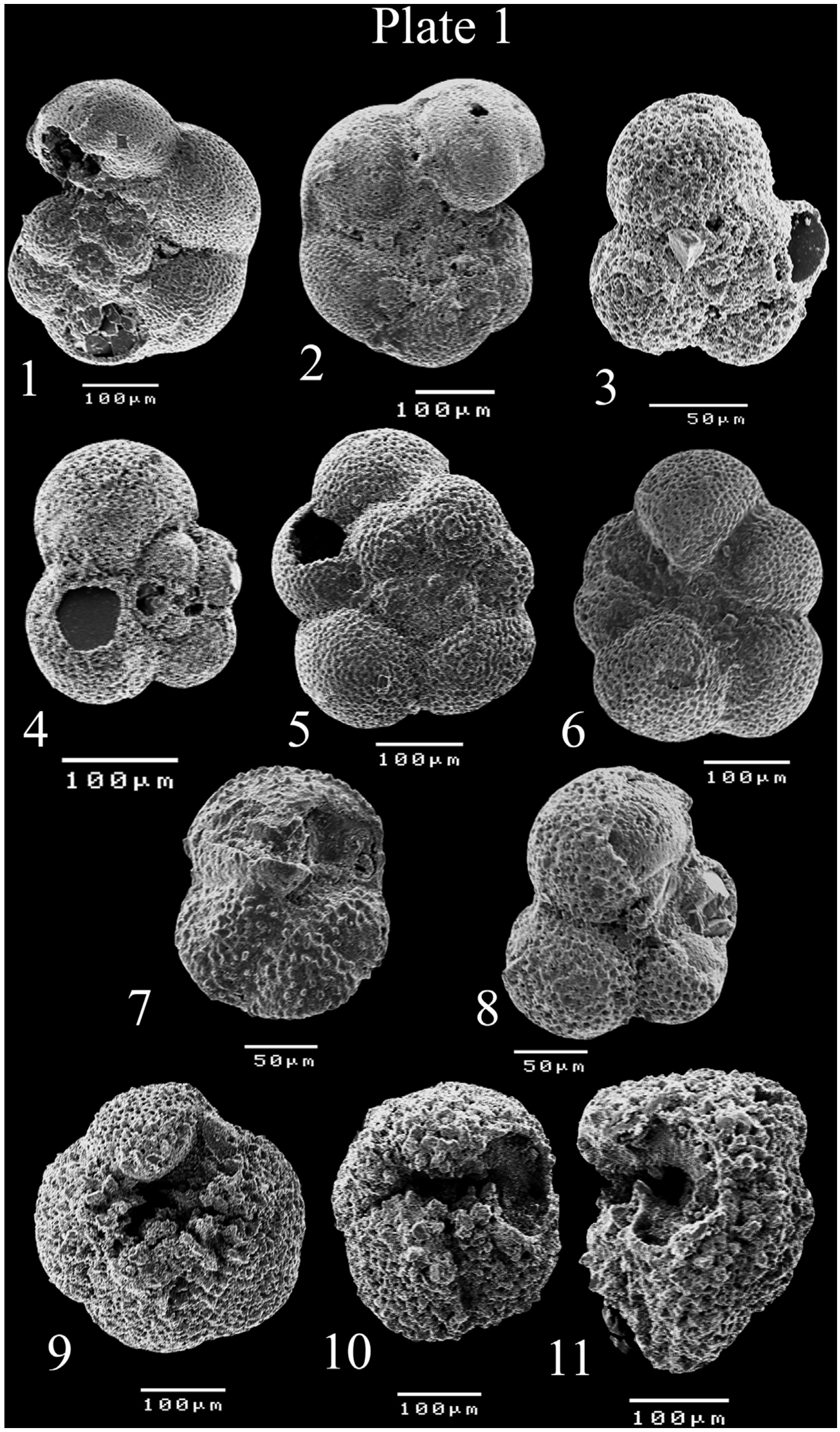

Plate 1. Shows the dissolution susceptibility of some planktonic foraminifera genera. 1, 2- *Pseudohastegerina wilcoxensis* (Cushman and Ponton), 1- dorsal view, 2-ventral view, sample 66, North Gunna section; 3, 4- *Parasubbotina variospira* (Belford), sample 59, North Gunna section; 5, 6- *Praemurica inconstans* (Subbotina), 5- dorsal view, 6- ventral view, sample 59, North Gunna section; 7- *Igorina albeari* (Cushman and Bermúdez), sample 32, North Gunna section; 8- *Subbotina cancellata* (Blow), sample 62, North Gunna section; 9- *Acarinina subsphaerica* (Subbotina), sample 58, North Gunna section; 10, 11- *Acarinina coalingensis* (Cushman and Hanna), 10-ventral view, 11- side view, sample 61, North Gunna section.

L. pseudomamilligera, *Dentalina eocenica*, *Nodosaria redicula, Lagena striata*, *Bolivinopsis spectablis*, *Vaginulinopsis austinana*, *Loxostomum tegulatum*, *Globobulimina suteri*, *Bulimina inflate, Cibicidoides pharaonis, Cibicidoides succedens* and *Anomalinoides umboniferus* (Table 5).

Similarly, the fourth interval of carbonate dissolution is represented by high content of arenaceous forms as the underlying sample 66 of third interval with addition the presence of *Gaudryina rectiangulata*, *Gaudryina rudita*, *Gaudryina elegantissima* and *Spiroplectammina dentata*.

Generally the following criteria within the four intervals bed are potential indicators of dissolution: 1) low P/B ratios; 2) low

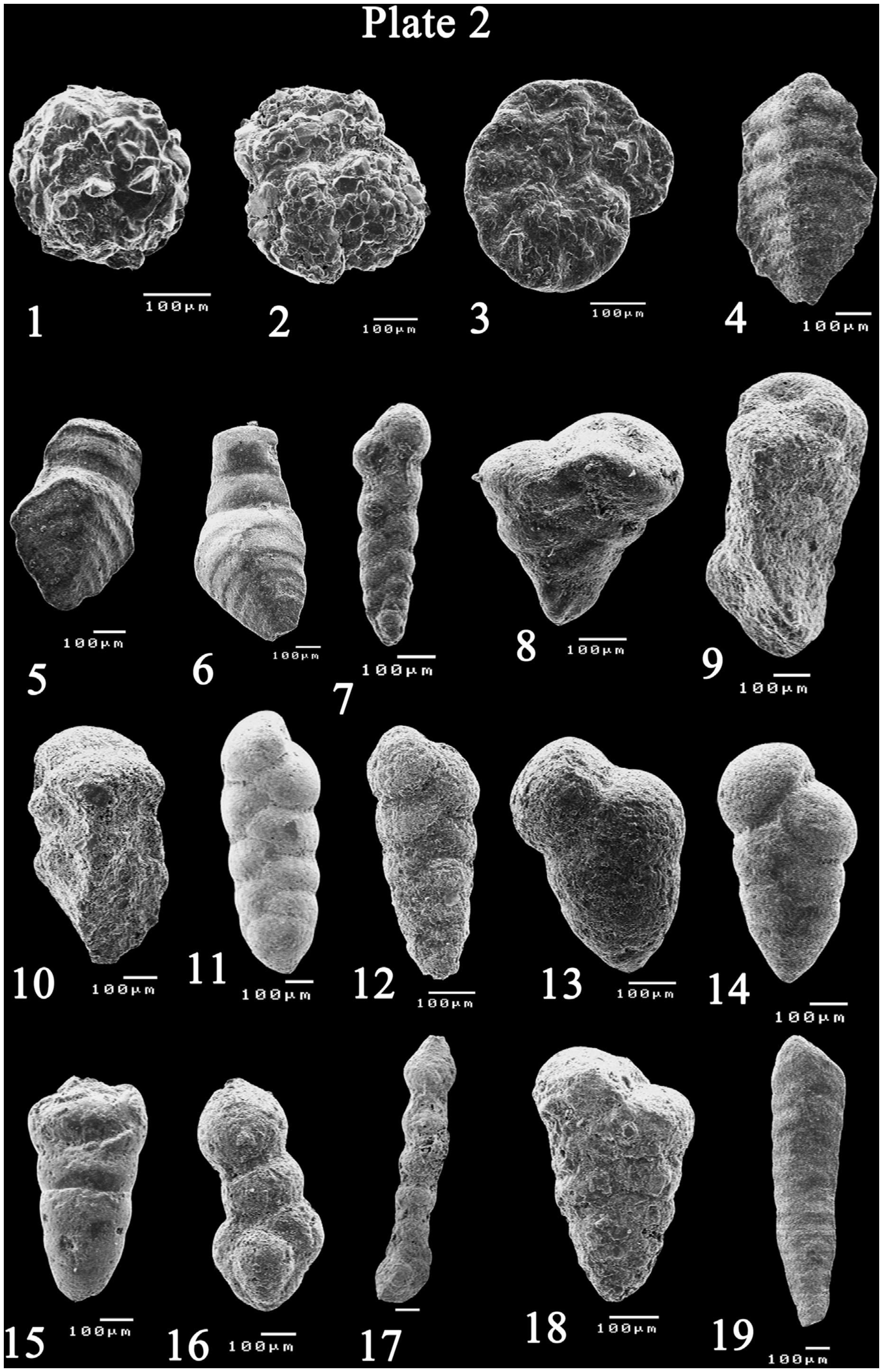

Plate 2. Shows the agglutinated foraminifera species occurred at the four intervals of dissolution. 1- *Psammosphaera fusca* SCHULTZE, 1875, sample 14; 2- *Trochammina uniatensis* TAPPAN; 1988, sample 11; 3-*Haplophragmoides excavatus* CUSHMAN and WATERS, 1927, sample 5; 4- *Spiroplectammina dentata* (ALTH, 1850), sample 12; 5- *Vulvulina colei* CUSHMAN, 1932, sample 22; 6- *Vulvulina advena* CUSHMAN, 1948, sample 59; 7-*Gaudryina elegantissima* SAID and KENAWY, 1956, sample 63; 8-*Gaudryina rectiangulata* TEN DAM AND SIGAL, 1950, sample 66; 9-*Gaudryina rudita* SANDIDGE, 1932, sample 69; 10-*Gaudryina soldadoensis* CUSHMAN and RENZ, 1942, sample 26; 11-*Migros midwayensis* (PARR, 1935), sample 12; 12-*Dorothia bulletta* (CARSEY, 1926), sample 10; 13-*Dorothia conulus* (REUSS, 1845), sample 19; 14-*Dorothia glabrella* CUSHMAN, 1933, sample 3; 15- *Marsonella oxycona* (REUSS, 1860), sample 70; 16-*Pseudoclavulina amorpha* CUSHMAN, 1926, sample 61; 17-*Pseudoclavulina globulifera* (TEN DAM and SIGAL, 1950), sample 11; 18-*Textularia punjabensis* HAQUE, 1956, sample 6; 19-*Textularia* cf. *plummerae* LALICKER, 1935, sample 50.

foraminiferal numbers; 3) high relative abundance of the non-calcareous agglutinated taxa; 4) high relative abundance of calcareous taxa resistant to dissolution, especially *Lenticulina*; 5) low relative abundance of susceptible calcareous taxa, such as unilocular, uniserial and biserial taxa for the benthics and non-muricate taxa for the planktonics; and 6) low simple diversity, which coincide with the observation of Nguyen and Speijer (2014).

Four inferred carbonate dissolution intervals are recognized at the Dakhla and Esna formations of the Farafra Oasis of Egypt; 1) at the Danian/Selandian boundary, 2) at the upper part of *Acarinina*

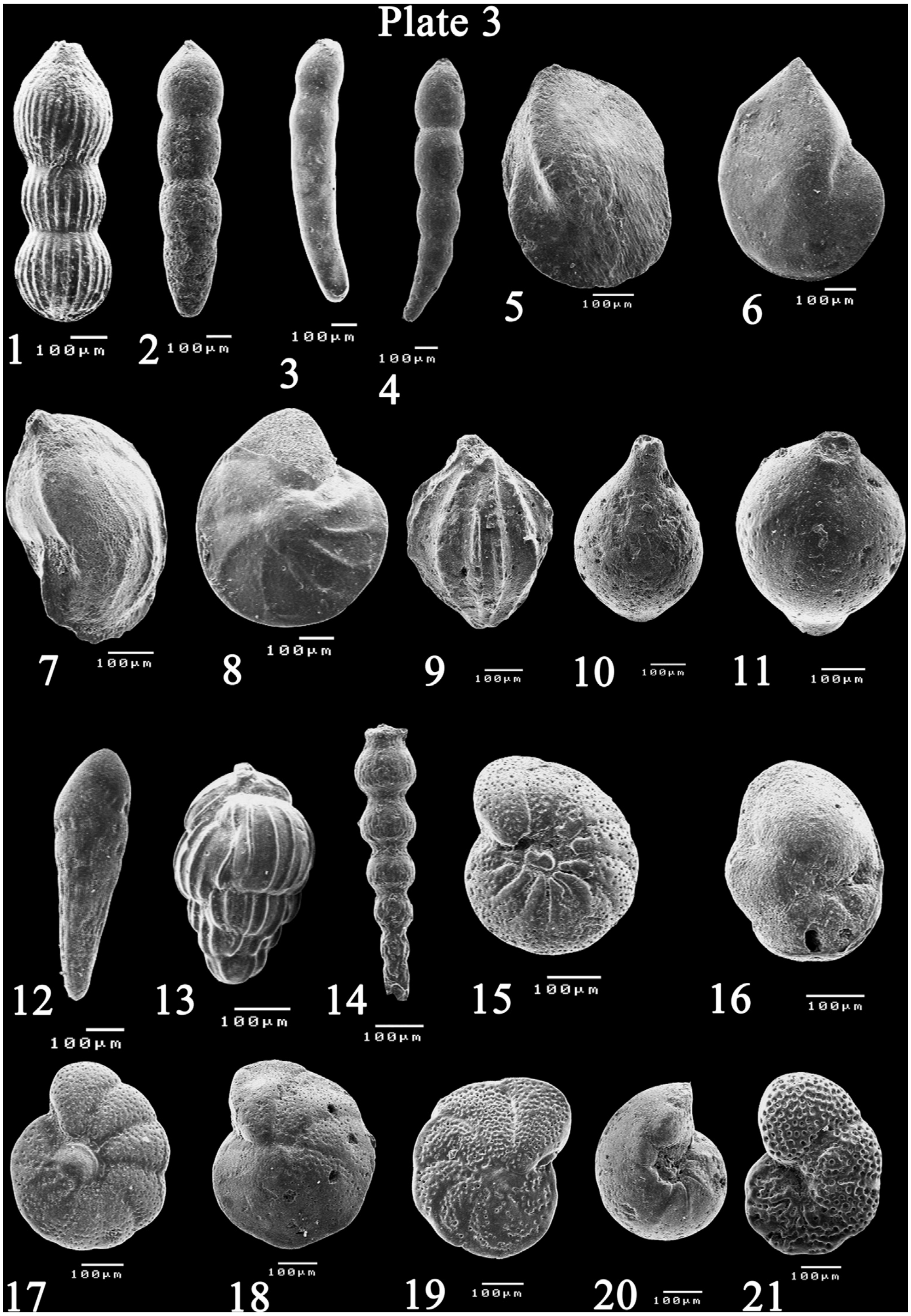

Plate 3. Shows some calcareous foraminifera species occurred at the four intervals of dissolution. 1- *Nodosaria limbata* D'Orbigny, 1932, Sample 65; 2- *Nodosaria redicula* (LINNE, 1956), Sample 68; 3- *Dentalina colei* CUSHMAN and DUSENBURY, Sample 27; 4- *Dentalina eocenica* CUSHMAN, 1966, Sample 63; 5- *Lenticulina navicula* (SCHWAGER, 1883), Sample 65; 6- *Lenticulina pseudomamilligera* (PLUMMER, 1927), Sample 68; 7- *Lenticulina oligostegia* (REUSS, 1860), Sample 58; 8- *Lenticulina midwayensis* (PLUMMER, 1927), Sample 58; 9- *Lagena sulcata* (WALKER and JACOB, 1798), Sample 68; 10- *Lagena apiculata* (REUSS, 1851), Sample 22; 11- *Lagena globosa* (MONTAGU, 1803), Sample 20; 12- *Loxostomum tegulatum* (REUSS, 1845), Sample 26; 13- *Bulimina inflate* (KENNETT, 1966), Sample 14; 14- *Stilostomella midwayensis* (CUSHMAN and TODD, 1946), Sample 26; 15- *Cibicidoides abudurbensis* (NAKKADY, 1950), Sample 68; 16- *Cancris auricular* (EITCHTEL and MOLL, 1798), Sample 58; 17- *Anomalinoides umboniferus* (SCHWAGER, 1883), Sample 66; 18- *Cibicidoides pharaonis* (LEROY, 1953), Sample 66; 19- *Cibicidoides praecursoria* SCHWAGER, 1883, Sample 63; 20- *Gyroidinoides subangulata* (PLUMMER, 1927), Sample 50; 21- *Anomalinoides granosa* BROTZEN, 1945, Sample 62.

soldadensis P4c Biozone, 3) at the upper two third of the *Morozvella velascoensis* P5 Biozone and 4) at the Paleocene/Eocene boundary (P5/E5). These intervals are characterized by high percentages of non-calcareous agglutinated taxa (Fig. 4) (Table 1).

6. Faunal patterns

1 The benthic foraminiferal assemblage of the Danian/Selandian (P3a/P3b) is characterized by the richness of arenaceous

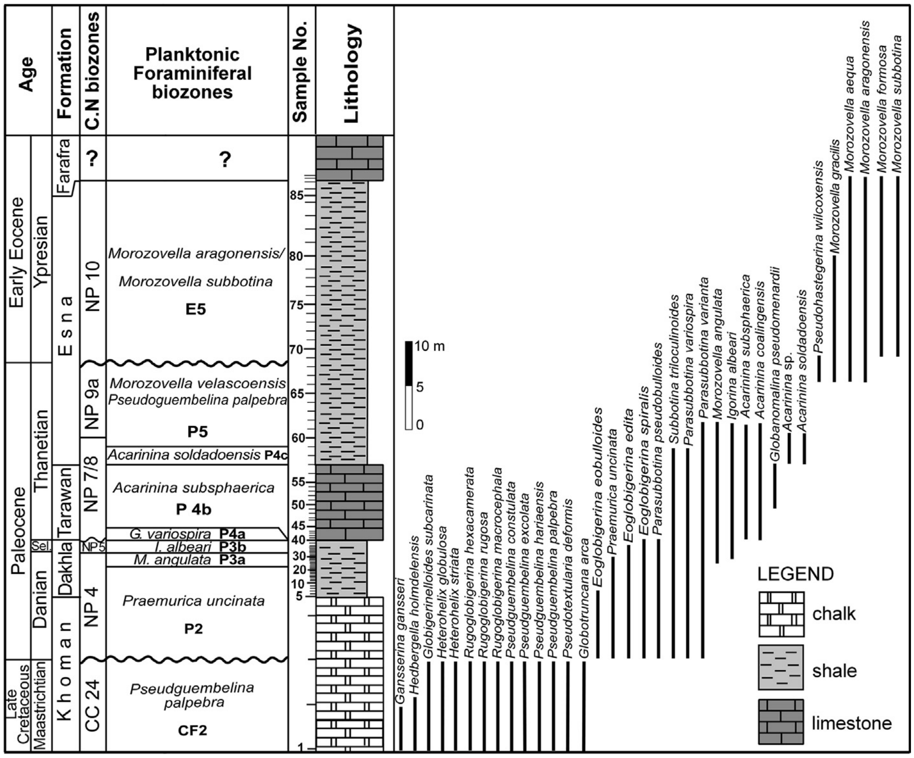

Fig. 3. Range chart of the common planktonic foraminiferal species in North Gunna section, Farafra Oasis, Egypt.

Table 2
Calcareous benthic foraminiferal species counts in the studied samples from P3a Biozone of the first interval of dissolution.

Calcareous Benthic Foraminifera	Sample no.								
	20	21	22	23	24	25	26	27	28–32 Barren
Lagena apiculata	12	11	14	–	–	–	2	–	–
Stilostomella gracillima	14	–	47	58	20	–	21	9	–
Gyroidinoides subangulata	–	–	–	–	–	–	3	–	–
Cibicidoides praecursoria	47	–	87	89	40	–	50	22	–
Total	73	11	148	147	60	–	76	31	–

foraminifera as *Dorothia conulus*, *Vulvulina colei*, *Migros midwayensis*, *G. soldadoensis*, *P. amorpha* and *P. globulifera*, where the top of P3a Biozone is barren from foraminifera.

2 The planktonic taxa, in the upper part of *A. soldadoensis* Biozone (P4c) and in *M. velascoensis* Biozone (P5), *Subbotina*, *Acarinina* and *Morozovella* are the major components of the planktonic assemblages, whereas *Igorina*, *Parasubbotina* and *Globanomalina* constitute just minor parts (Fig. 5).

3 For the benthic taxa, the few presences of *L. apiculata* and *L. striata* (uniloculars), *S. gracillima* and *D. eocenica* (uniserial), *Loxostomum tegulatum* (biserial) respectively indicate they are most dissolution susceptible in the four intervals recognized in the studied section (Tables 2–5). Meanwhile, the most resistant group is composed of trochospirals and planispirals as indicated by high numbers of *L. pseudomamilligera*, *L. oligostegia*, *C. praecursoria*, *A. umboniferus* and *A. affinis.*

Table 3
Calcareous benthic foraminiferal species counts in the studied samples from P4c Biozone of the second interval of dissolution.

Calcareous Benthic Foraminifera	Sample no.		
	57	58	59 Barren
Lenticulina pseudomamilligera	33	15	–
Lenticulina oligostegia	24	18	–
Anomalinoides affinis	21	22	–
Gyroidinoides subangulata	18	–	–
Stilostomella gracillima	4	–	–
Total	100	55	–

7. Discussion

1 The quantitative studies in the four intervals shows that the unilocular are the most dissolution vulnerable followed by the uniserial and biserial groups (Fig. 6). The two spiral groups are the most dissolution resistant. Particularly robust planispiral and trochospiral taxa are *Lenticulina, Cibicidoides* and *Anomalinoides.* These findings are in line with other quantitative studies (e.g., Douglas, 1973; Martin et al., 1995; Yasuhara et al., 2012). Accordingly, the planispiral *Lenticulina* is documented to be the most dissolution resistant taxa, whereas rotaliines

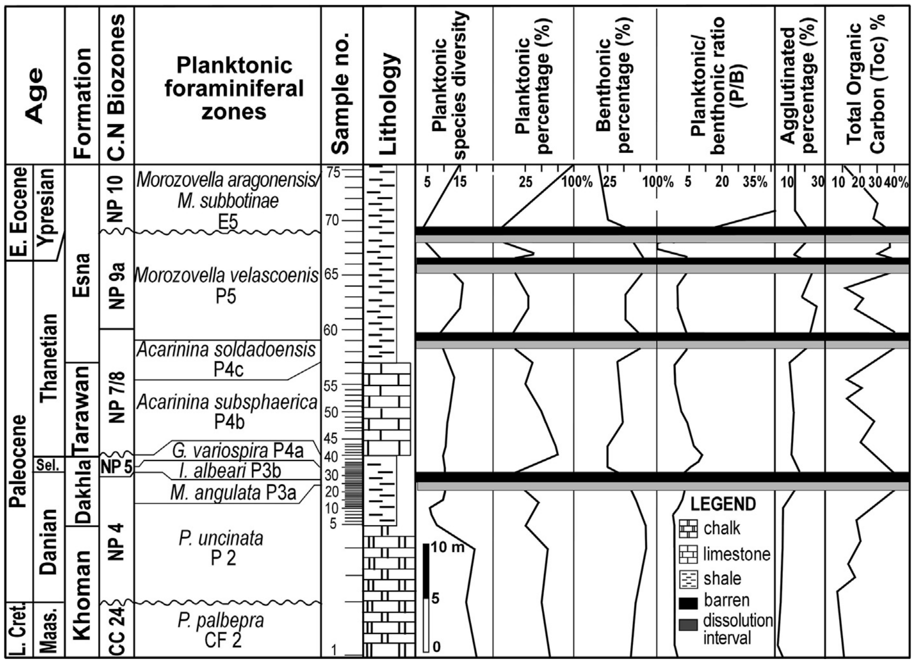

Fig. 4. The dissolution intervals of planktonic foraminifera in North Gunna section.

such as *Cibicidoides* and *Anomalinoides* have an intermediate susceptibility and biserial hyaline taxa are the most susceptible (Nguyen et al., 2009; Nguyen and Spijer, 2014).

2 In the four intervals the high relative abundances of agglutinated taxa suggesting that these intervals have experienced severe dissolution. The faunas consisting entirely or dominantly of agglutinated forms is attributed to brackish environments or stagnant conditions (Løfaldli and Nagy, 1980; Nagy et al., 1988, 1990). The increased organic carbon together with the virtually agglutinated nature of the assemblages imply that the depositional beds of these intervals experienced dysaerobic bottom conditions with lower PH. Such conditions would exclude calcareous assemblages, which were presumably less tolerant of dysoxia and low PH than agglutinated faunas (e.g., Phleger, 1960; Murray, 1967, 1973; Bradshaw, 1968).

3 At the fourth dissolution intervals the relative decrease of the planktonic foraminiferal number (PFN) compared to the benthic one (BFN) (Table 1), leads to a decrease of P/B ratios, depressed abundance of *Subbotina*, or increased abundance of *Lenticulina* (e.g., Canudo et al., 1995; Lu et al., 1998) that are potentially indicative of dissolution. The dissolution of the foraminiferal assemblage indicates that planktonics are generally more vulnerable to dissolution than benthics (e.g., Thunell, 1976; Thunell and Honjo, 1981; Metzler et al., 1982; Peterson and Prell, 1985; Dittert et al., 1999). Berger (1973) estimated that benthic foraminifera are on the average approximately three

Table 4
Calcareous benthic foraminiferal species counts in the studied samples from the upper two third of P5 Biozone of the third interval of dissolution.

Calcareous benthic foraminifera	Sample no.							
	60	61	62	63	64	65	66	67 Barren
Gyroidinoides girardanus	7	–	2	4	–	3	–	–
Siphogerenoides eleganta	2	–	–	–	–	–	–	–
Stilostomella midwayensis	–	–	3	–	–	6	–	–
Stilostomella gracillima	–	–	1	–	–	3	–	–
Valvulineria scrobiculata	1	–	1	–	–	–	–	–
Cibicidoides pharaonis	4	3	4	5	–	7	13	–
Cibicidoides succedens	6	4	8	12	–	8	3	–
Lagena apiculata	–	3	3	6	–	3	–	–
Lagena sulcata	–	4	5	8	–	1	–	–
Astacolus gryi	3	2	–	3	–	–	–	–
Astacolus bifurcatus i	2	1	–	2	–	–	4	–
Vaginulinopsis austinana	–	–	3	4	–	–	–	–
Loxostomum tegulatum	–	7	4	6	–	4	–	–
Loxostomum applinae,	–	3	6	8	–	–	–	–
Pullenia quinqueloba	–	–	1	2	–	–	–	–
Stainforthia farafraensis	–	–	3	2	–	–	–	–
Lenticulina pseudomamilligera	7	7	12	15	4	12	9	–
Lenticulina oligostegia	5	3	3	5	–	3	11	–
Bulimina inflate	2	–	–	–	–	–	–	–
Anomalinoides cf. *acutus*	7	4	9	14	–	9	7	–
Anomalinoides umboniferus	5	3	3	8	–	6	16	–
Anomalinoides ekblomi	3	2	4	10	–	4	8	–
Osangularia plummerae	–	3	7	1	–	4	5	–
Total	54	46	82	115	4	73	76	–

Table 5
Calcareous benthic foraminiferal species counts in the studied samples from the upper most of P5 Biozone of the fourth interval of dissolution.

Calcareous benthic foraminifera	Sample no.	
	68	69 Barren
Lagena striata	5	–
Bolivinopsis spectablis	2	–
Vaginulinopsis austinana	4	–
Loxostomum tegulatum	5	–
Dentalina eocenica	5	–
Nodosaria redicula	9	
Bulimina inflate	3	–
Globobulimina suteri	2	–
Lenticulina pseudomamilligera	12	–
Lenticulina oligostegia	10	–
Cibicidoides pharaonis	10	
Cibicidoides succedens	7	
Anomalinoides umboniferus	15	–
Total	89	–

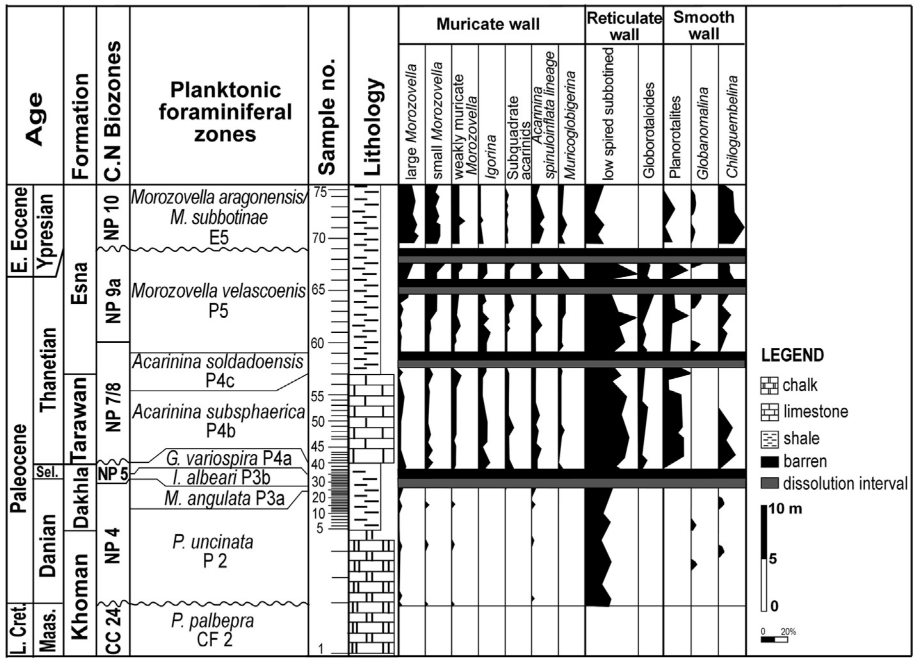

Fig. 5. Planktonic foraminiferal biozonation, relative population abundances of species from the Paleocene of North Gunna section.

times less susceptible to calcite dissolution than planktonics (Fig. 7).

4 The benthic foraminiferal assemblage of the Danian/Selandian (P3a/P3b) is characterized by the richness of arenaceous foraminifera. The presence of glauconitic beds (sample 28–30) at the base of *I. albeari* (P3b) Biozone associated with the high percentage of TOC is marked by declination in P/B ratio and increase in agglutinated percentage (Fig. 4). At these beds the benthic are dominated by shallow forams (e.g., *Dorothia*, *Lenticulina* and *Anomalinoides*) and the high contents of organic matters, which dissolved planktonic calcareous foraminiferal tests. Glauconite is generally, associated with slow deposition, under reducing conditions on the continental margin and facilitated by presence of organic matter (Reading, 1986).

5 Among to the planktonic foraminifera of Paleocene taxa, the results confirm previous experimental results on differential dissolution susceptibility at generic level (Nguyen et al., 2009). Accordingly, the large muricate *Acarinina* and *Morozovella* are most resistant, followed by the cancellate *Subbotina* and the muricate *Igorina* (Quillévéré and Norris, 2003) (Fig. 5). At species level, the thick-walled *A. soldadoensis, A. subsphaerica*, and the large *M. subbotinae* are the most resistant species. Most of the large *Morozovella* species such as *M. aequa*, *M. angulata* and *M. aragonensis*, together with *A. subsphaerica P. variospira, Subbotina cancellata* show average dissolution resistance.

8. Summary and conclusion

Four inferred carbonate dissolution intervals are recognized in the Farafra Oasis of Egypt; 1) at the Danian/Selandian boundary of the Dakhla Formation (P3a/P3b), 2) at the upper part of *A.*

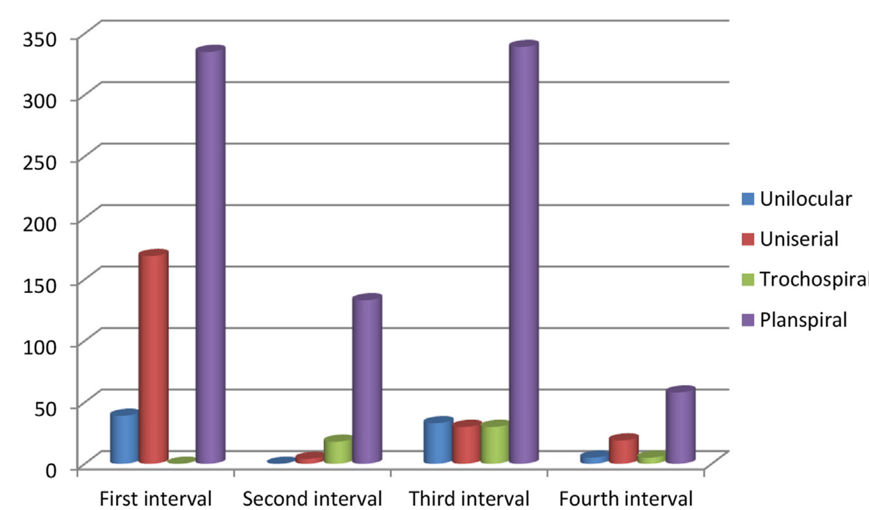

Fig. 6. Shows the distribution of number of specimens belonging to each architectural type of calcareous benthic foraminifera in different intervals.

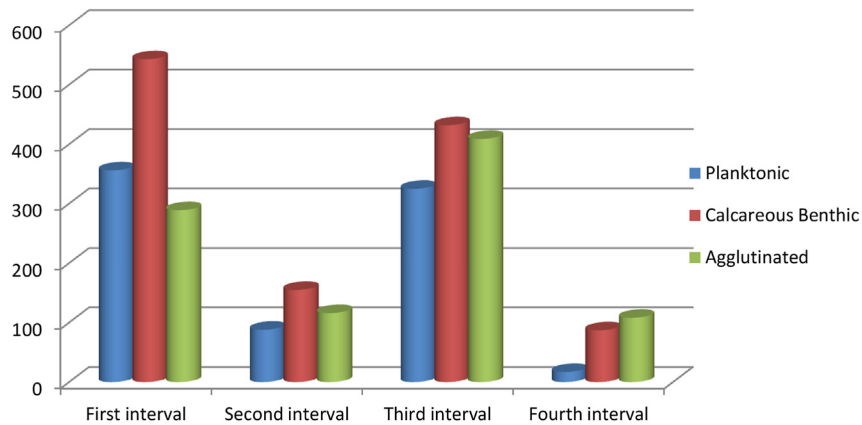

Fig. 7. Shows the distribution of number of planktonic, calcareous benthic and agglutinated specimens in different intervals.

soldadoensis/Globanomalina pseudomenardii Subzone (P4c ((Early Thanetian), 3) at the upper two third part of the *Morozvella velascoenis* (P5) biozone (Latest Thanetian) and 4) at the Paleocene/Eocene boundary of *M. velascoensis/Morozovella aragonensis-M. subbotinae* (P5/E5) of the Esna Formation. These intervals are characterized by high absolute numbers of calcareous benthic foraminifera and high percentages of non-calcareous agglutinated taxa. The statistical analysis of planktonic foraminifera of North Gunna section confirms *Subbotina* and *Parasubbotina* are the most dissolution-susceptible taxon in the studied assemblages, whereas *Acarinina* and *Morozovella* are less dissolution-prone.

The presence of glauconitic beds at the base of *I. albeari* (P3b) Biozone associated with the high percentage of TOC of the upper part of the Dakhla Formation is marked by declination in P/B ratio and increase in agglutinated percentage. At these beds the high contents of organic matters dissolved planktonic foraminiferal tests. Glauconite is generally, associated with slow deposition, under reducing conditions on the continental margin and facilitated by presence of organic matter.

The few presences of *L. apiculata* and *L. striata* (unioculars), *S. gracillima* and *D. eocenica* (uniserial), *Loxostomum tegulatum* (biserial) respectively indicate they are most dissolution susceptible in the four intervals recognized in the studied section. Meanwhile, the most resistant group is composed of trochospirals and planispirals as indicated by high numbers of *L. pseudomamilligera*, *L. oligostegia, C. praecursoria*, *Anomalinoides umboniferus* and *A. affinis*.

References

Awad, G.H., Ghobrial, M.G., 1965. Zonal Stratigraphy of the Kharga Oasis. In: Min. Indu., Gen. Egy. Org. Geol. Res. Min., Geol. Sur., Cairo, vol. 34, pp. 1–77.

Arz, J.A., Molina, E., 2002. Bioestratigrafíay cronoestratigrafía con foraminíferos planctónicos del Campaniense superior y Maastrichtiense de latitudes subtropicales y templadas (España, Francia, y Tunicia). Neues Jahrb. Für Geol. Paläontologie Abh. 224, 161–195.

Barthel, K.W., Herrmann-Degen, W., 1981. Late Cretaceous and early tertiary stratigraphy in the Great Sand Sea and its SE margins (Farafra and Dakhla oases), SW desert, Egypt. Mitt. Bayer. Staatsslg. Palaont. Hist. Geol. 21, 141–182.

Beadnell, H.J.L., 1905. The Topography and Geology of the Fayum Province of Egypt. Egypt. Surv. Dept., Cairo, 101.

Berger, W.H., 1967. Foraminifera ooze, solution at depth. Science 156 (3773), 383–385.

Berger, W.H., 1970. Planktonic foraminifera-selective solution and lysocline. Mar. Geol. 8 (2), 111–138.

Berger, W.H., 1973. Deep-sea carbonates: Pleistocene dissolution cycles. J. Foraminifer. Res. 3, 187–195.

Berger, W.H., Diester-Haass, L., 1988. Paleoproductivity: the benthic planktonic ratio in foraminifera as a productivity index. Mar. Geol. 81 (1–4), 15–25.

Berggren, W.A., Pearson, P.N., 2005. A revised tropical to Subtropical paleogene planktonic foraminiferal zonation. J. Foraminifer. Res. 35, 279–298.

Berggren, W.A., Kent, D.V., Swisher III, C.C., Aubry, M.-P., 1995. A revised Cenozoic geochronology and chronostratigraphy. In: Berggren, W.A., Kent, D.V., Hardenbol, J. (Eds.), Geochronology, Time Scales and Global Stratigraphic Correlations: A Unified Temporal Framework for an Historical Geology. Society of Economic Paleontologists and Mineralogists Special Publication, vol. 54, pp. 129–212. Tulsa.

Berner, R.A., Berner, E.K., Keir, R.S., 1976. Aragonite dissolution on Bermuda pedestal-its depth and geochemical significance. Earth Planet. Sci. Lett. 30 (2), 169–178.

Bradshaw, J.S., 1968. Environmental parameters and marsh Foraminifera. Limnol. Oceanogr. 13, 26–30.

Canudo, J.I., Keller, G., Molina, E., Ortiz, N., 1995. Planktic foraminiferal turnover and δ13C isotopes across the Paleocene–Eocene transition at Caravaca and Zumaya, Spain. Palaeogeogr. Palaeoclimatol. Palaeoecol. 114 (1), 75–100.

Casieri, S., Carboni, M.G., 2007. Late Quaternary paleoenvironmental reconstruction of San Benedetto Del Tronto coast (central Adriatic Sea) by benthic foraminiferal assemblages. Geol. Romana 40, 163–173.

Corliss, B.H., 1979. Size variation in the deep sea benthic foraminifera Globocassidulina subglobosa (Brady) in the Southern Indian Ocean. J. Foraminifer. Res. 9 (1), 50–60.

Corliss, B.H., Honjo, S., 1981. Dissolution of deep-sea benthonic foraminifera. Micropaleontology 27 (4), 356–378.

Caron, M., 1985. Cretaceous planktic foraminifera, in Plankton stratigraphy. In: Bolli, H.M., Sautiders, J.B., Perch-Nielsen, K. (Eds.). Cambridge Univ. Press., Cambridge., 17-86.

Dittert, N., Baumann, K.H., Bickert, T., Henrich, R., Huber, R., Kinkel, H., Meggers, H., 1999. Carbonate dissolution in the deep-sea: methods, quantification and paleoceanographic application. In: Fischer, G., Wefer, G. (Eds.), Use of Proxies in Paleoceanography: Examples from the South Atlantic. Springer-Verlag, Berlin Heidelberg, pp. 255–284.

Douglas, R.G., 1973. Benthonic foraminiferal biostratigraphy in the Central North Pacific Leg 17, deep sea Drilling Project. In: Winterer, E.L., Ewing, J.I. (Eds.), Deep Sea Drilling Project. Initial Reports 17 (Available from: World Wide Web: http://deepseadrilling.org/17/volume/dsdp17–21.pdf.

El-Akkad, S., Issawi, B., 1963. Geology and iron ore deposits of the Bahariya Oasis. Egy. Geol. Surv. Min. Res. Dep. Pap. 18, 1–301.

Guasti, E., Kouwenhoven, T.J., Brinkhuis, H., Speijer, R.P., 2005. Paleocene sea-level and productivity changes at the southern Tethyan margin (El Kef, Tunisia). Mar. Micropaleontol. 55 (1–2), 1–17.

Herrero, C., Canales, M.L., 2002. Taphonomic processes in selected Lower and Middle Jurassic foraminifera from the Iberian range and Basque-Cantabrian Basin (Spain). J. Foraminifer. Res. 32 (1), 22–42.

Issawi, B., El-Hinnawi, M., Francis, M., Mazhar, A., 1999. The Phanerozoic Geology of Egypt a Geodynamic Approach. Special Publication No.76. The Egyptian Geological Survey.

Li, L., Keller, G., 1998a. Maastrichtian climate, productivity and faunal turnover in planktic foraminifera in south Atlantic DSDP Sites 525 A and 21. Mar. Micropaleontol. 33, 5–86.

Li, L., Keller, G., 1998b. Abrupt deep-sea warming at the end of the Cretaceous. Geology 26, 995–998.

Li, L., Keller, G., Stinnesbeck, W., 1999. The Late Campanian and Maastrichtian in northwestern Tunisia: paleoenvironmental inferences from lithology, macrofauna and benthic foraminifera. Cretac. Res. 20, 231–252.

Løfaldli, M., Nagy, J., 1980. Foraminiferal stratigraphy of Jurassic deposits on Kongsøya, Svalbard. Skr. Nor. Polarinst 172, 63–96.

Lu, G., Keller, G., Pardo, A., 1998. Stability and change in Tethyan planktic foraminifera across the Paleocene–Eocene transition. Mar. Micropaleontol. 35 (3–4), 203–233.

Malak, E.K., Philobos, A., Ashry, M.M., 1977. Some petrographical, mineralogical and organic geochemical characteristics of black shales from Quseir and Safaga, Red Sea Area, Egypt. Desert Inst. Bull. ARE 27, 1–15.

Martin, R.E., Harris, M.S., Liddell, W.D., 1995. Taphonomy and time averaging of foraminiferal assemblages in Holocene tidal flat sediments, Bahia la Choya, Sonora, Mexico (northern Gulf of California). Mar. Micropaleontol. 26 (1–4), 187–206.

Metzler, C.V., Wenkam, C.R., Berger, W.H., 1982. Dissolution of foraminifera in the Eastern Equatorial Pacific-an in situ experiment. J. Foraminifer. Res. 12 (4), 362–368.

Murray, J.W., 1967. Living foraminiferids of tidal marshes- a review. J. Foram. Res. 1, 153–161 (New York).

Murray, J.W., 1973. Distribution and Ecology of Living Benthic Foraminiferids. Heinemann Educ. Book, London, 274p.

Nagy, J., Løfaldli, M., Bäckström, S.A., 1988. Aspects of foraminiferal distribution and depositional conditions in Middle Jurassic to Early Cretaceous shales in eastern Spits Bergen. In: Rögl, F., Gradstein, F.M. (Eds.), Second Workshop Agglutinated Foraminifera, 30. Abhandlungen der geologischen Bundesanstalt, Wien, pp. 287–300.

Nagy, J., Pilskog, B., Wilhelmsen, R., 1990. Facies controlled distribution of foraminifera in the Jurassic North Sea Basin. In: Hemleben, C., et al. (Eds.), Paleoecology, Biostratigraphy, Paleoceanography and Taxonomy of Agglutinated Foraminifera. NATO ASI Series C327. Kluwer Academic Publishers, pp. 621–657.

Nguyen, T.M.P., Petrizzo, M.R., Speijer, R.P., 2009. Experimental dissolution of a fossil foraminiferal assemblage (Paleocene-Eocene Thermal Maximum, Dababiya, Egypt): implications for paleoenvironmental reconstructions. Mar. Micropaleontol. 73, 241–258.

Nguyen, T.M.P., Speijer, R.P., 2014. A new procedure to assess dissolution based on experiments on Pliocene-Quaternary foraminifera (ODP Leg 160, Eratosthenes Seamount, Eastern Mediterranean). Mar. Micropaleontol. 106, 22–38.

Nolet, G.J., Corliss, B.H., 1990. Benthic foraminiferal evidence for reduced deep-water circulation during sapropel deposition in the eastern Mediterranean. Mar. Geol. 94 (1–2), 109–130.

Peterson, L.C., Prell, W.L., 1985. Carbonate dissolution in recent sediments of the eastern equatorial Indian Ocean: preservation patterns and carbonate loss above the lysocline. Mar. Geol. 64 (3–4), 259–290.

Petrizzo, M.R., Leoni, G., Speijer, R.P., De Bernardi, B., Felletti, F., 2008. Dissolution susceptibility of some paleogene planktonic foraminifera from ODP site 1209 (Shatsky Rise, Pacific ocean). J. Foraminifer. Res. 38 (4), 357–371.

Phleger, F.B., 1960. Foraminiferal population in Laguna Madre, Texas. Sci. Rep. Tohoku Univ. Spec. 4, 83–91 (Tohoku).

Quillévéré, F., Norris, R.D., 2003. Ecological development of acarininids (planktonic foraminifera) and hydrographic evolution of Paleocene surface waters. In: Wing, S.L., et al. (Eds.), Causes and Consequences of Globally Warm Climates in the Early Paleogene, 369. The Geological Society of America, Boulder, Colorado, pp. 223–238.

Reading, H.G. (Ed.), 1986. Sedimentary Environments and Facies. Blackwell scientific publications, Oxford, 615 pp.

Said, R., 1962. The Geology of Egypt. Elsevier, Amsterdam, 377.

Schlanger, S.O., Douglas, R.G., 1973. Porosity and textural changes related to the ooze-chalk-limestone transition. Eur. Geophys. Soc. Meet. Abstr. 1, 92.

Speijer, R.P., Schmitz, B., 1998. A benthic foraminiferal record of Paleocene sea level and trophic/redox conditions at Gebel Aweina, Egypt. Palaeogeogr. Palaeoclimatol. Palaeoecol. 137 (1–2), 79–101.

Stephen, P.B., Buzas, M.A., 2005. Population dynamics and dissolution of foraminifera in Nueces Bay, Texas. J. Foraminifer. Res. 35 (3), 248–258.

Tobin, R., Scott, D.B., Collins, E.S., Medioli, F.S., 2005. Infaunal benthic foraminifera in some North American marshes and their influence on fossil assemblages. J. Foraminifer. Res. 35 (2), 130–147.

Thunell, R.C., 1976. Optimum indices of calcium carbonate dissolution in deep-sea sediments. Geology 4 (9), 525–528.

Thunell, R.C., Honjo, S., 1981. Calcite dissolution and the modification of planktonic foraminiferal assemblages. Mar. Micropaleontol. 6 (2), 169–182.

de Vernal, A., Bilodeau, G., Hillairemarcel, C., Kassou, N., 1992. Quantitative assessment of carbonate dissolution in marine sediments from foraminiferlinings vs shell ratios. Davis Strait, Northwest North-Atlantic. Geology 20 (6), 527–530.

Yasuhara, M., Hunt, G., Cronin, T.M., Hokanishi, N., Kawahata, H., Tsujimoto, A., Ishitake, M., 2012. Climatic forcing of Quaternary deep-sea benthic communities in the North Pacific Ocean. Paleobiology 38 (1), 162–179.